Theory of Microwave-Assisted Supercurrent in Diffusive SNS Junctions

Pauli Virtanen,[1] Tero T. Heikkilä,[1] F. Sebastián Bergeret,[2,3,4] and Juan Carlos Cuevas[2]

[1]*Low Temperature Laboratory, Aalto University School of Science and Technology, P.O. Box 15100, FI-00076 AALTO, Finland*
[2]*Departamento de Física Teórica de la Materia Condensada, Universidad Autónoma de Madrid, E-28049 Madrid, Spain*
[3]*Centro de Física de Materiales (CFM), Centro Mixto CSIC-UPV/EHU, Edificio Korta, Avenida de Tolosa 72, E-20018 San Sebastián, Spain*
[4]*Donostia International Physics Center (DIPC), Manuel de Lardizbal 4, E-20018 San Sebastián, Spain*

(Received 24 January 2010; published 17 June 2010)

The observation of very large microwave-enhanced critical currents in superconductor–normal-metal–superconductor (SNS) junctions at temperatures well below the critical temperature of the electrodes has remained without a satisfactory theoretical explanation for more than three decades. Here we present a theory of the supercurrent in diffusive SNS junctions under microwave irradiation based on the quasiclassical Green's function formalism. We show that the enhancement of the critical current is due to the energy redistribution of the quasiparticles in the normal wire induced by the electromagnetic field. The theory provides predictions across a wide range of temperatures, frequencies, and radiation powers, both for the critical current and the current-phase relationship.

DOI: 10.1103/PhysRevLett.104.247003 PACS numbers: 74.45.+c, 74.25.N−, 74.50.+r

It was predicted by Eliashberg already in 1970 [1] that the condensation energy of a superconducting thin film can be increased by irradiating the film with microwaves. Within the framework of his theory, one can explain the small microwave-induced increase of the critical current of superconducting bridges for temperatures very close to the critical temperature [2–4], which is known as the Dayem-Wyatt effect. In the context of diffusive superconductor–normal-metal–superconductor (SNS) junctions, several experiments have shown that upon irradiation the critical current can be enhanced by up to several orders of magnitude [5,6]. This occurs even at temperatures well below the critical temperature of the superconducting electrodes, which cannot be understood in terms of stimulation of superconductivity in the leads. Additionally, these experiments show that the critical current is a nonlinear function of the radiation power, which existing linear response theories [7,8] cannot explain.

There is now renewed interest in this problem, triggered by recent experiments. Fuechsle *et al.* [9] measured the current-phase relationship under microwave irradiation, and reported that the current is progressively suppressed at phase differences close to π as the radiation amplitude increases. Moreover, Chiodi *et al.* [10] observed that critical current is enhanced when the microwave frequency is larger than the inverse diffusion time in the normal metal. Besides, there are many recent device suggestions utilizing SNS junctions in the presence of high-frequency fields, such as those used in metrology [11] and in radiation detection [12].

To understand the microwave-assisted supercurrent in diffusive SNS junctions, we develop a microscopic theory based on the quasiclassical Keldysh-Usadel approach, which takes into account the nonlinear effects of the microwave irradiation. Our theory provides a quantitative description for a wide range of values of the temperature, microwave power, frequency, and the strength of inelastic scattering. In particular, we show that the large enhancement of the critical current originates from the presence of a minigap, E_g, in the density of states of the normal wire. This minigap blocks some of the transitions caused by the microwave radiation, which results in a redistribution of quasiparticles, enhancing the supercurrent when the temperature T is comparable or larger than E_g/k_B. We also show that the nonequilibrium distribution in the normal wire leads to a highly nonsinusoidal current-phase relationship, in good agreement with Ref. [9].

We consider a diffusive normal metal (N) of length L connecting two bulk superconductors with energy gap Δ [see inset of Fig. 1(b)]. In the absence of microwaves, superconducting pair correlations leak into the normal metal modifying its properties. For instance, the local density of states (DOS) is modulated [13] and a supercurrent can flow through the normal metal [14]. The DOS exhibits a minigap $E_g(\varphi)$, see Fig. 1(a), which depends on the superconducting phase difference φ [15]. In this work we focus on the long-junction limit, where the Thouless energy $E_T = \hbar D/L^2$ (D is the diffusion constant) is much smaller than Δ, as appropriate for the experiments [5,6,9,10]. In this case and for ideal interfaces, which we consider hereafter, $E_g(0) \approx 3.12E_T$, whereas $E_g(\pi) = 0$.

We model the microwave radiation by an oscillating electric field, $\vec{E}(t)$, described by a time-dependent vector potential $\vec{A}(t) = \vec{A}_0 \cos(\omega_0 t)$, where $\vec{A}_0$ points along the axis of the junction. We neglect screening, and assume that the field is position independent [16]. We also neglect the effect of the radiation inside the superconductors, which is justified for frequencies smaller than $\Delta/\hbar$ or when the electrodes are thick compared to the size of the junction. To evaluate the physical observables, we use the quasi-

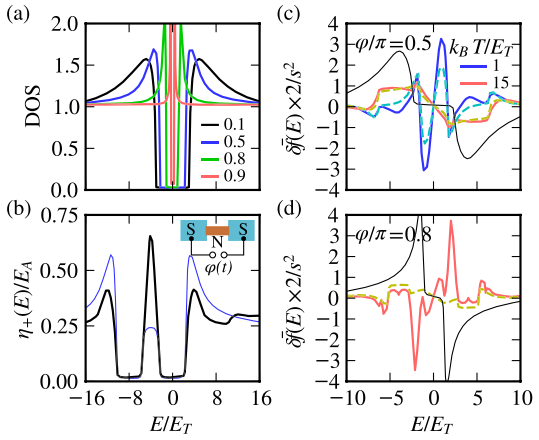

FIG. 1 (color online). (a) Local density of states (DOS) in the middle of the normal wire for $\Delta = 100E_T$ and different values of the phase difference φ/π, in the absence of microwaves. (b) Absorption rate η_+ for a high frequency $\hbar\omega_0/E_T = 8$ and $\varphi = \pi/2$, $s = 0.125$. Thin line shows the approximation from Eq. (4). Inset: Schematic representation of the SNS junction. (c) Correction $\delta\bar{f} = \bar{f} - f_0$ to the electron distribution function vs energy at two different temperatures for $\varphi = \pi/2$, $\hbar\omega_0/E_T = 4$, and $s = 0.125$. Solid lines correspond to the exact numerical results and the dashed lines to the approximation in Eq. (4). The thin black line shows the spectral supercurrent $j_S(E)$ in the absence of microwaves. (d) The same as in (c) for $k_BT/E_T = 15$ and $\varphi = 0.8\pi$.

classical theory of superconductivity for diffusive systems [18,19]. It is formulated in terms of momentum averaged Green functions $\check{G}(\vec{R}, t, t')$ which depend on position $\vec{R}$ and two time arguments. These propagators are 4×4 matrices in Keldysh $\otimes$ Nambu space:

$$\check{G} = \begin{pmatrix} \hat{G}^R & \hat{G}^K \\ 0 & \hat{G}^A \end{pmatrix}, \qquad \hat{G}^R = \begin{pmatrix} g^R & f^R \\ \tilde{f}^R & \tilde{g}^R \end{pmatrix}. \tag{1}$$

Here, $\hat{G}^{R,A,K}$ are the retarded, advanced and Keldysh components, respectively. The Green functions acquire the BCS value $\check{G}_0(t - t', \pm\varphi/2)$ inside the superconductors, and in the normal metal fulfill the Usadel equation

$$\hbar D\hat{\nabla} \circ (\check{G} \circ \hat{\nabla} \circ \check{G}) = [-i\epsilon\hat{\tau}_3 + i\check{\sigma}, \check{G}]_0, \tag{2}$$

where $\circ$ denotes the time convolution $(X \circ Y)(t, t') = \int_{-\infty}^{\infty} dt_1 X(t, t_1) Y(t_1, t')$, $\hat{\nabla}$ the gauge-invariant gradient $\hat{\nabla} \circ X = \nabla X - i[e\vec{A}\hat{\tau}_3/\hbar, X]_\circ$ which involves the vector potential $\vec{A}(t, t') = \vec{A}(t)\delta(t - t')$, and $\epsilon(t, t') = i\hbar\partial_t\delta(t - t')$. The self-energy $\check{\sigma}$ describes inelastic interactions in the wire, and the Green functions are normalized as $(\check{G} \circ \check{G})(t, t') = \delta(t - t')$.

Because Andreev reflection blocks subgap heat transport out of the junction, inelastic interactions play an important role in balancing the energy brought into the junction by the microwaves. We describe these interactions, for example due to phonons, within the relaxation time approximation, where the interaction strength is characterized by a constant energy (scattering rate) Γ [17]. The microwave coupling, in turn, introduces the energy scale $E_A = e^2DA_0^2/\hbar$. One can show that the ratio $s^2 = E_A/E_T$ determines the change in the spectral quantities due to the microwaves, while the ratio $\alpha = E_A/\Gamma$ controls the corresponding change in the electron distribution. We note that $s = eV_0/\hbar\omega_0$, where V_0 is the amplitude of the oscillating voltage across the junction.

In order to solve Eq. (2), we follow Ref. [20] and Fourier transform the Green functions to energy space. Because of the time dependence of the vector potential, the Usadel equation in energy space admits a solution of the type $\check{G}(\mathbf{R}, E, E') = \sum_m \check{G}_{0,m}(\mathbf{R}, E)\delta(E - E' + m\hbar\omega_0)$. With this ansatz the Usadel equation becomes a set of coupled differential equations for the Fourier components $\check{G}_{n,m}(E) = G(E + n\hbar\omega_0, E + m\hbar\omega_0)$. Below, we denote the Fourier components of all variables with similar subscripts. For arbitrary radiation power we solve these equations numerically [17]. From the solution of $\check{G}$, we can compute all physical observables.

We now analyze the linear response regime (s^2, $\alpha \ll 1$). In this limit, we can derive the kinetic equation for the time average of the distribution function, $\bar{f}$, by keeping terms up to the second order in A_0 in the Keldysh component of the Usadel Eq. (1). Because of Andreev reflection, when relaxation processes are slower than the diffusion inside the junction, $\bar{f}$ is in our gauge constant throughout the normal wire. Consequently, the kinetic equation reduces to an equality of the electron-phonon and microwave collision integrals, $I_{\text{e-ph}} = I_\gamma$, averaged over the junction volume Ω. The microwave collision integral resembles Joule heating and it is proportional to a time-averaged product of electric field and current (at energy E), $I_\gamma = \frac{eD}{8\omega_0}\overline{\vec{E}(t) \cdot \mathrm{Tr}\hat{\tau}_3\hat{j}^K(E + \hbar\omega_0/2, t)} - (E \mapsto E - \hbar\omega_0)$, where $\hat{j}^K = \hat{G}^R \circ \hat{\nabla} \circ \hat{G}^K + \hat{G}^K \circ \hat{\nabla} \circ \hat{G}^A$. Using this result [17], the kinetic equation for the correction $\delta\bar{f} = \bar{f} - f_0$, where f_0 is the Fermi function, becomes

$$\begin{aligned}\Gamma\langle\rho\rangle\delta\bar{f} = {} & \eta_-(E + \hbar\omega_0)f_+(1 - f_0) - \eta_+(E)f_0(1 - f_+) \\ & + \eta_+(E - \hbar\omega_0)f_-(1 - f_0) - \eta_-(E)f_0(1 - f_-).\end{aligned} \tag{3}$$

Here, $\langle\rho\rangle$ is the spatially averaged DOS inside the junction and $f_\pm = f_0(E \pm \hbar\omega_0)$. The emission ($\eta_-$) and absorption ($\eta_+$) rates are defined as $\eta_+(E) = \eta_-(E + \hbar\omega_0) = -\frac{eDA_0}{16}\,\mathrm{Im}\,\mathrm{Tr}\hat{\tau}_3\langle\hat{j}^K_{0,1}(E)\rangle/[f_0(E + \hbar\omega_0) - f_0(E)]$.

For frequencies $\hbar\omega_0 < 2E_g(\varphi)$, one can neglect the ac components of the retarded and advanced functions, so that

$$\eta_+ \approx \frac{E_A}{4}\left\langle \rho_0\rho_+ + \frac{1}{4}\,\mathrm{Re}\{(f_0^R + \tilde{f}_0^{R*})(\tilde{f}_+^R + f_+^{R*})\}\right\rangle. \tag{4}$$

This reduces to the original linear response result by Eliashberg in the case of a bulk superconducting film [1]. One can now see that the minigap in ρ and f^R blocks some

of the radiation-induced transitions [see Fig. 1(b)]. Thus, if the temperature is sufficiently high [$k_BT \gtrsim E_g(\varphi)$], an excess of quasiparticles accumulates below the minigap, and their number is depleted above it. This cooling effect is illustrated in Fig. 1(c), where the result of (4) is compared to the exact numerical result. As one can see, Eq. (4) reproduces the main features of the exact result well especially at $k_BT \gg E_g(\phi)$. Note that despite the cooling at some energies, the Joule power absorbed in the junction, $P = \nu_F \int dEE\Omega\langle I_\gamma\rangle = \overline{I(t)V(t)}$ where ν_F is the normal-state DOS, is positive.

However, Eq. (4) does not describe correctly the behavior of the distribution function when $\hbar\omega_0 > 2E_g(\varphi)$, as shown in Fig. 1(d). This means that Eq. (4) always fails to describe the behavior close to $\varphi = \pi$. In this limit, the radiation induces changes in the ac components of the retarded and advanced quantities that couple to the time-averaged distribution function, especially at energies close to $E = \pm\hbar\omega_0/2$. Since the behavior of these components is determined by a complicated balance between diffusion and ac excitation, an accurate description of $\eta_\pm$ in general requires a numerical calculation.

In the limit $\Gamma \ll E_T$, the correction to the supercurrent I_S comes mainly from the change in the distribution function, and it can be written as

$$\delta I_S \approx \frac{S\sigma_N}{e}\int_{-\infty}^{\infty} dEj_S(E)\delta\bar{f}(E), \tag{5}$$

where S is the cross section, $\sigma_N = e^2\nu_F D$ the normal-state conductivity of the wire and $j_S(E)$ the equilibrium spectral supercurrent [21], which is plotted in Figs. 1(c) and 1(d) together with $\delta\bar{f}$. Based on this, the cooling effect described by Eq. (4) is expected to manifest as an enhancement of the critical current for $k_BT \gtrsim E_g(0)$. This is confirmed by the exact numerical calculations obtained in the low-amplitude regime, see Fig. 2. The effect increases up to frequency $\hbar\omega_0 \approx 2E_g(0)$, and at larger frequencies becomes more varying, due to the complicated energy dependence of j_S and $\bar{f}$. On the other hand, as Γ increases, the magnitude of $\delta\bar{f}$ decreases, which together with the suppression of the minigap and j_S reduces the current. The above is in qualitative agreement with existing experiments [5,6], which concentrated on $\hbar\omega_0/E_T \lesssim 10$.

For high power, the magnitude of the critical current eventually decreases as can be seen in Fig. 3. This occurs as large-amplitude oscillations of the phase average the density of states, which results in a suppression of the coherence and in the subsequent closing of the minigap [see Fig. 4(a)]. As a consequence, the cooling effect is suppressed, and microwaves mainly heat the electrons in the same way as in the normal state, which reduces the current. In the relaxation time approximation the temperature is for high field strength given by $T^* \approx [P/(2\nu_F\Omega k_B^2\Gamma_0)]^{1/5}$ (provided $T \lesssim T^* \ll \Delta/k_B$ and assuming $\Gamma(T) = 4\Gamma_0T^3$ [22]), where $P = \sigma_N\Omega A_0^2\omega_0^2/2$ is the average Joule power dissipated in the junction.

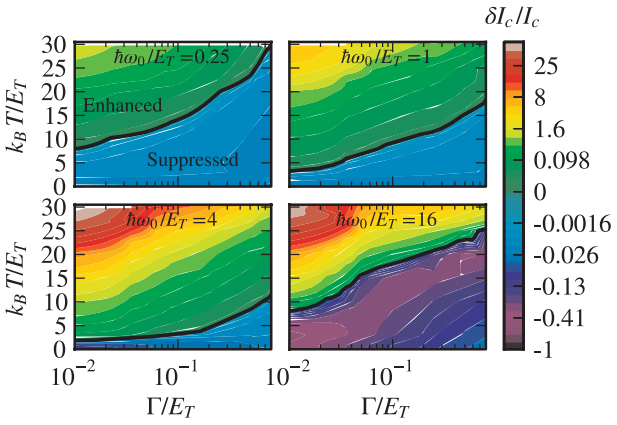

FIG. 2 (color). Correction to the critical current, normalized by the critical current in the absence of the field, as a function of temperature and inelastic rate for $\Delta = 100E_T$ and several frequencies. The field strength is $s = 0.125$ in all cases. The lines separate the region of parameters for which the critical current is enhanced from that in which it is reduced.

The critical current also exhibits oscillations when radiation amplitude increases, see Fig. 3(a), similar to those already seen in the early experiments [5,6]. For short junctions ($\Delta < E_T$; not plotted), we find that these oscillations match reasonably well with the usual Bessel oscillations in Josephson tunnel junctions, i.e., $I \propto J_0(2s)$, but in the long-junction limit the similarity is only qualitative. Locations of the dips in the $I_c(s)$ relation are not strongly dependent on the temperature, but depend on the radiation frequency, as shown in Fig. 3(b).

The microwave irradiation alters the current-phase relationship, enhancing the current at $\varphi \lesssim \frac{\pi}{2}$ and suppressing it or even changing its sign at $\varphi \gtrsim \frac{\pi}{2}$ [see Fig. 4(b)]. The behavior near $\varphi = \pi$ comes from two sources: the cooling disappears as the minigap closes, and the features peculiar

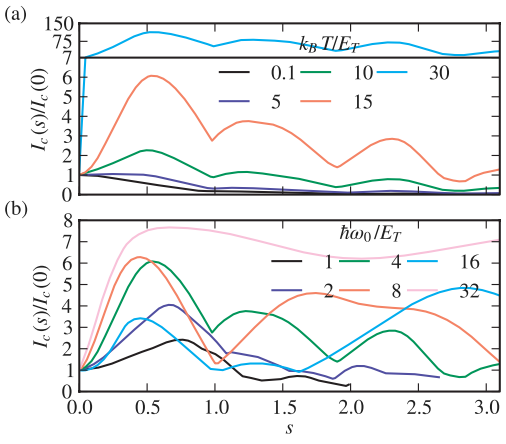

FIG. 3 (color online). Critical current (normalized by the current without ac field at the corresponding temperature) versus radiation amplitude s for a wire with $\Delta/E_T = 100$. (a) For different temperatures at $\hbar\omega_0/E_T = 4$ and $\Gamma/E_T = 0.05$. (b) For different frequencies and $k_BT/E_T = 15$.

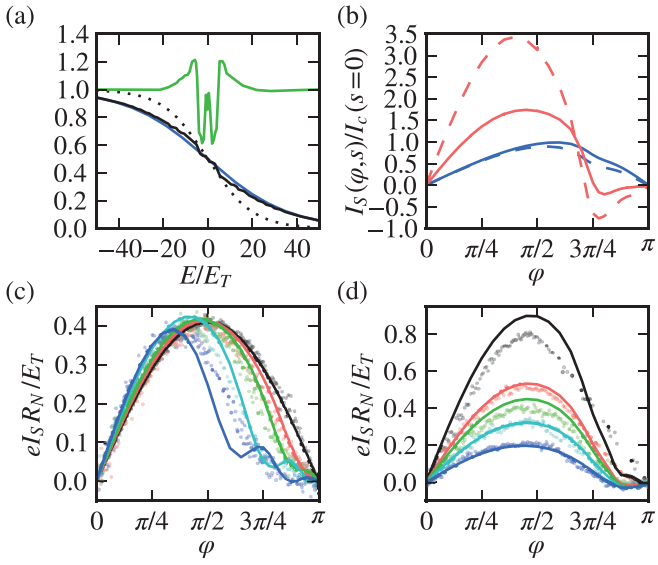

FIG. 4 (color). (a) Distribution function (solid black) and density of states (green) for large amplitude $s = 2$, and $\hbar\omega_0/E_T = 4$, $\Delta/E_T = 100$, $k_BT/E_T = 10$, $\Gamma/E_T = 0.05$, and $\varphi = \pi/2$. Microwaves cause heating from $k_BT/E_T = 10$ (dotted) to $k_BT \approx \hbar\omega_0\sqrt{E_A/4\Gamma}$ (blue). (b) Current-phase relation normalized to equilibrium critical current at $k_BT/E_T = 15$, 1 (top to bottom) and $s = 0.125$ (solid) and 0.25 (dashed), for $\hbar\omega_0/E_T = 4$, $\Delta/E_T = 100$, $\Gamma/E_T = 0.05$. (c) Current-phase relation for different amplitudes $s = 0$, 0.2, 0.3, 0.5, 0.75 (solid, top to bottom) at $k_BT/E_T = 10$ and $\hbar\omega_0/E_T = 1.2$. Relaxation rate is chosen as $\Gamma/E_T = 0.2(k_BT/10E_T)^3$, and $\Delta/E_T = 58$. Experimental data from Ref. [9] are shown as dots. (d) As in (c), for $s = 0.3$, $\hbar\omega_0/E_T = 2$, and temperatures $k_BT/E_T = 8$, 9.5, 10, 11, 12.5 (top to bottom).

to the dissipative ac response of SNS junctions not contained in Eq. (4) become increasingly important.

To compare with the results of Ref. [9], we compute the current-phase relationship using the parameters (T, E_T, ω_0) of the experiment. We have two free parameters: Γ/E_T, which we assume large enough to suppress the enhancement of the critical current, and the amplitude of the ac bias, which we fix by assuming that $s = 0.5$ corresponds to the externally applied power level 28 dBm at $\hbar\omega_0/E_T = 1.2$. The power dependence, see Fig. 4(c), reproduces the main experimental features: (i) with increasing power the maximum supercurrent is reached at $\varphi_{\max} < \pi/2$, (ii) I_S is strongly suppressed for phases close to π, and (iii) for $\varphi < \varphi_{\max}$, I_S is slightly enhanced compared to $s = 0$. On the other hand, as shown in Fig. 4(d), the deviation from the sinusoidal form becomes slightly more pronounced as T increases, in qualitative agreement with experiments. The difference to the experiment at high power or low temperatures may be due to nonlinear radiation coupling and the relaxation time approximation, respectively.

In summary, we have presented a general theory for describing the effects of radiation on the properties of diffusive SNS junctions, which explains a wide range of experimental observations. We have clarified the mechanism of stimulated superconductivity, shown how the supercurrent depends on the field strength nonmonotonically, and predicted the modification of the current-phase relation. Moreover, our results pave the way for filling some remaining gaps in the understanding of SNS junction physics such as the finite-voltage Shapiro steps [14] or the role of phase fluctuations providing the "intrinsic shunting" [11], as both phenomena require describing the junctions in the presence of a finite-frequency driving.

We thank Christoph Strunk, Marco Aprili, Teun Klapwijk and Yuli Nazarov for discussions, and CSC (Espoo) for computer resources. This work was supported by the Spanish MICINN (Contract No. FIS2008-04209), EC funded ULTI Project Transnational Access in Programme FP6 (Contract No. RITA-CT-2003-505313). F. S. B. acknowledges funding by the Ramón y Cajal program and T. T. H. the funding by the Academy of Finland and the ERC (Grant No. 240362-Heattronics).

[1] G. M. Eliashberg, JETP Lett. **11**, 114 (1970).
[2] A. F. G. Wyatt *et al.*, Phys. Rev. Lett. **16**, 1166 (1966).
[3] A. H. Dayem and J. J. Wiegand, Phys. Rev. **155**, 419 (1967).
[4] T. Klapwijk, J. van den Bergh, and J. Mooij, J. Low Temp. Phys. **26**, 385 (1977).
[5] H. A. Notarys, M. L. Yu, and J. E. Mercereau, Phys. Rev. Lett. **30**, 743 (1973).
[6] J. M. Warlaumont *et al.*, Phys. Rev. Lett. **43**, 169 (1979).
[7] L. G. Aslamazov and S. Lempitskii, Sov. Phys. JETP **55**, 967 (1982).
[8] A. Zaikin, Sov. Phys. JETP **57**, 910 (1983).
[9] M. Fuechsle *et al.*, Phys. Rev. Lett. **102**, 127001 (2009).
[10] F. Chiodi, M. Aprili, and B. Reulet, Phys. Rev. Lett. **103**, 177002 (2009).
[11] S. P. Benz *et al.*, Appl. Phys. Lett. **71**, 1866 (1997).
[12] F. Giazotto *et al.*, Appl. Phys. Lett. **92**, 162507 (2008).
[13] H. le Sueur *et al.*, Phys. Rev. Lett. **100**, 197002 (2008).
[14] P. Dubos *et al.*, Phys. Rev. B **63**, 064502 (2001).
[15] F. Zhou *et al.*, J. Low Temp. Phys. **110**, 841 (1998).
[16] Electric field can be assumed constant in normal structures thinner than the skin depth, which is realistic for our parameters. As explained in [17], proximity effect induces a small but finite scalar potential, which however does not significantly affect our results.
[17] See supplementary material at http://link.aps.org/supplemental/10.1103/PhysRevLett.104.247003.
[18] K. D. Usadel, Phys. Rev. Lett. **25**, 507 (1970).
[19] A. I. Larkin and Y. N. Ovchinnikov, in *Nonequilibrium Superconductivity*, edited by D. Langenberg and A. Larkin (Elsevier, Amsterdam, 1986), p. 493.
[20] J. C. Cuevas *et al.*, Phys. Rev. B **73**, 184505 (2006).
[21] T. T. Heikkilä, J. Särkkä, and F. K. Wilhelm, Phys. Rev. B **66**, 184513 (2002).
[22] This corresponds to electron-phonon coupling, see for example J. Rammer, *Quantum Transport Theory* (Perseus Books, Reading, MA, 1998).